

# **Stimulated Radiation Interaction of a Single Electron Quantum Wavepacket**

Avraham Gover, Yiming Pan

*Department of Electrical Engineering Physical Electronics,*

*Tel Aviv University, Ramat Aviv 69978, ISRAEL*

## **Abstract**

We analyze the stimulated (emission/absorption) interaction of a single electron quantum wavepacket with coherent radiation, using perturbation theory and numerical solution of Schrodinger equation. The analysis applies to a wide class of free electron radiative interaction schemes, and exemplified for Smith-Purcell radiation. Though QED theory and experiments indicate that spontaneous emission of radiation by a free electron is independent of its dimensions, we show that the wavepacket dimensions do affect the stimulated radiative interaction in a certain range. We identify two different operating ranges: When the drift length is long, wavepacket phase and dimension-dependent acceleration/deceleration is fundamentally impossible because of the wavepacket spread. For short drift, such acceleration is possible, and there we bridge the transition to classical “point particle” linear acceleration, corresponding to a wavepacket, short relative to the radiation wavelength. An independent quantum effect is the significance of the quantum recoil in stimulated radiative interaction. The quantum analysis emulates the results of FEL theory in the quantum regime, on one hand, and of quantum momentum recoil sidebands in PINEM on the other hand. We use the platform for discussing the fundamental physics question of measurability of the quantum wavepacket size.

When interacting with a radiation wave under the influence of an external force, free electrons can emit radiation spontaneously, or be stimulated to emit/absorb radiation and get decelerated/accelerated. Such an interaction can also be facilitated without an external force when the electron passes through polarizable medium. Numerous spontaneous radiative emission schemes of both kinds are well known: Synchrotron radiation, Undulator radiation, Compton Scattering, Cerenkov radiation, Smith-Purcell radiation, transition radiation [1-6]. Some of these schemes were demonstrated to operate as coherent stimulated radiative emission sources, such as Free Electron Lasers (FEL) [7-9], as well as accelerating (stimulated absorption) devices, such as Dielectric Laser Accelerator (Inverse Smith-Purcell effect) [10]. In principle, all free electron spontaneous radiation emission schemes can be turned into stimulated emission devices, because of the fundamental Einstein relations between spontaneous emission and stimulated emission/absorption [11].

All of these spontaneous and stimulated radiation schemes have been analyzed in the classical limit - where they are modeled as point particles, and in the quantum limit - where they are normally modeled as plane waves [11-12]. Though some electron wavepacket features were considered in the context of infinite interaction length spontaneous Cerenkov radiation emission [13-14] there is no existing quantum wavepacket theory of stimulated radiative interaction that encompasses the quantum plane wave limit, the classical point particle limit and the intermediated finite wavepacket regime.

The interpretation and the essence of the electron quantum wavepacket and its electromagnetic interactions have been a subject of confusion and debate since the early conception of quantum mechanics. Modern QED theory and experiments indicate that spontaneous emission by a free electron is independent of its wavepacket dimensions [15-20]. However, in the present paper we focus on the stimulated emission process, and show that the wavepacket dimensions do affect the interaction in a certain range of operation.

The finite wavepacket, finite interaction length model presented here for free electron stimulated radiative interaction, leads to a distinction between two kinds of quantum effect conditions in single electron interaction: “the quantum recoil condition” and “the wavepacket significance condition”. The first condition relates to the significance of the electron quantum recoil relative to the momentum uncertainty in a finite interaction length. The second condition relates to whether the electrons interact with the radiation as a point particle with a determined phase or as an extended wave. This condition, contrary to common experience, assigns significance to the wavepacket size at the time of the radiative interaction and the history of its generation and transport to the interaction region.

Our one-dimensional interaction model is based on the first order perturbation solution of the relativistic “modified Schrödinger equation” [11]:

$$i\hbar \frac{\partial \psi(z, t)}{\partial t} = (H_0 + H_I(t))\psi(z, t), \quad (1)$$

where  $H_0 = p^2/2\gamma_0 m$  is the free space Hamiltonian, and the interaction part is:

$$H_I(t) = -\frac{e\hbar}{2\gamma_0 m\omega} \left\{ e^{-i(\omega t - \phi_0)} \tilde{E}(z) \cdot \nabla - e^{i(\omega t - \phi_0)} \tilde{E}^*(z) \cdot \nabla \right\}, \quad (2)$$

$$\tilde{E}(z) = E_0 e^{iq_z z} \hat{e}_z. \quad (3)$$

This model is fitting for discription of the variety of interaction schemes mentioned, where Equation (3) represents the dominant component of the radiation wave. We exemplify our modeling here for the case of Smith-Purcell radiation (see Figure 1), for which case the radiation wave is a Floquet mode:  $\tilde{E}(z) = \sum_m \tilde{E}_m e^{iq_{zm} z}$  with  $q_{zm} = q_{z0} + m2\pi/\lambda_G$ ,  $\lambda_G$  is the grating period,  $q_{z0} = q \cos \Theta$ ,  $q = \omega/c$  and  $\Theta$  is the incidence angle of the radiation wave relative to the axial interaction dimension. Equation (3) with  $q_z = q_{zm}$  represents one of the space harmonics  $m$  that satisfies synchronism

condition with the electron [6]:  $v_0 \cong \omega/q_{zm}$ . We note that the analysis would be similar for the Cerenkov interaction scheme with  $q_z = n(\omega)\cos\Theta$  and  $n(\omega)$  the index of reflection of the medium. Furthermore, the analysis can be straightforwardly extended to the case of FEL and other interaction schemes [11].

The solution of Schrodinger equation to zero order (i.e. free space propagation) is well known. Assuming that the initial wavepacket, which is emitted at some point  $z = -L_D$  near the cathode face at time  $t = -t_D$ , is a gaussian at its waist, then:

$$\psi^{(0)}(z, t) = \left(2\pi\sigma_{p_0}^2\right)^{-\frac{1}{4}} \int \frac{dp}{\sqrt{2\pi\hbar}} \exp\left(-\frac{(p-p_0)^2}{4\sigma_{p_0}^2}\right) e^{ip(z+L_D)/\hbar} e^{-iE_p(t+t_D)/\hbar} = \int \frac{dp}{\sqrt{2\pi\hbar}} c_p^{(0)} e^{-iE_p t/\hbar} |p\rangle, \quad (4)$$

where  $|p\rangle = e^{ipz/\hbar}$ . Note that  $L_D, t_D = L_D/v_0$  are the “effective” drift length and drift time of the wavepacket center, that are somewhat different from the geometric distance and drift time from the cathode face. This is because of the electron acceleration section and because the wavepacket longitudinal waist may be somewhere within the cathode.

Expanding the energy dispersion relation to second order

$$E_p = c\sqrt{m^2 c^2 + p^2} \approx E_0 + v_0(p - p_0) + \frac{(p - p_0)^2}{2m^*}, \quad (5)$$

The wavepacket development in momentum space is then given by

$$c_p^{(0)} = \left(2\pi\sigma_{p_0}^2\right)^{-\frac{1}{4}} \exp\left(-\frac{(p - p_0)^2}{4\tilde{\sigma}_p^2(t_D)}\right) e^{i(p_0 L_D - E_0 t_D)/\hbar}, \quad (6)$$

with

$$\tilde{\sigma}_p^2(t_D) = \sigma_{p_0}^2 \left(1 + i t_D / t_{R_{\parallel}}\right)^{-1}, \quad (7)$$

$$\sigma_{p_0} = \hbar / 2\sigma_{z_0}, \quad (8)$$

$$t_{R_{\parallel}} = \frac{m^* \hbar}{2\sigma_{p_0}^2} = 4\pi \frac{\sigma_{z_0}^2}{\lambda_c^* c}, \quad (9)$$

where  $m^* = m\gamma_0^3$  [4a] and we define

$$\lambda_c^* = \lambda_c / \gamma^3, \quad (10)$$

with  $\lambda_c = \hbar/mc$  – the Compton wavelength. The wavepacket development in space is calculated from Equation (4)

$$\psi^{(0)}(z, t) = \frac{\sqrt{\sigma_{z_0}}}{\left(2\pi\tilde{\sigma}_z^4(t+t_D)\right)^{1/4}} \exp\left(-\frac{(z-v_0 t)^2}{4\tilde{\sigma}_z^2(t+t_D)}\right) e^{i(p_0(z+L_D)-\varepsilon_0(t+t_D))/\hbar}, \quad (11)$$

where  $\tilde{\sigma}_z(t+t_D) = \sigma_{z_0} \sqrt{1+i(t+t_D)/t_{R_{\parallel}}}$ . Its probability distribution

$$\left|\psi^{(0)}(z, t)\right|^2 = \frac{1}{\sqrt{2\pi\sigma_z^2(t+t_D)}} \exp\left(-\frac{(z-v_0 t)^2}{2\sigma_z^2(t+t_D)}\right), \quad (12)$$

displays particle propagation at velocity  $v_0 = \beta_0 c = p_0/\gamma_0 m$  with wavepacket expansion:

$$\sigma_z(t) = |\tilde{\sigma}_z(t)| = \sigma_{z_0} \sqrt{1+t^2/t_{R_{\parallel}}^2}. \quad (13)$$

The parameter  $\tau$  (Equation (9)) is the evolution time from the waist for which  $\sigma_z(\tau) = \sqrt{2}\sigma_{z_0}$ , in analogy to the Rayleigh length of wave diffraction. We now solve Equation (1) using the first order perturbation theory in momentum space

$$\psi(z, t) = \psi^{(0)}(z, t) + \psi^{(1)}(z, t) = \int \frac{dp}{\sqrt{2\pi\hbar}} \left( c_p^{(0)} + c_p^{(1)} \right) e^{-iE_p t/\hbar} |p\rangle. \quad (14)$$

Integration of Equation (1) in momentum space for  $c_p^{(1)}$  produces energy conseving terms of single photon emission/absorption corresponding to the two terms in the perturbation Hamiltonian:

$$c_{p'}^{(1)(e,a)} = \frac{\pi}{2i\hbar} \int dp \langle p' | H_I^{(e,a)} | p \rangle c_p^{(0)} \delta\left(\frac{E_p - E_{p'} \mp \hbar\omega}{2\hbar}\right), \quad (15)$$

Expanding again the energy dispersion relation (5) to second order, the delta function determines the quantum momentum recoil

$$p_{rec}^{(e,a)} = \left| p^{(e,a)} - p \right| = \frac{\hbar\omega}{v_0} (1 \pm \delta), \quad (16)$$

where  $\delta = \frac{\hbar\omega}{2m^*v_0^2}$ . The first order perturbed coefficient is then

$$c_{p'}^{(1)(e,a)} = \frac{\pi}{iv_0} \langle p' | H_I^{(e,a)} | p \mp p_{rec}^{(e,a)} \rangle c^{(0)}(p \mp p_{rec}^{(e,a)}), \quad (17)$$

where the zero-order coefficient  $c_p^{(0)}$  is given in equation (6). The matrix element is straightforwardly calculated by

$$\begin{aligned} \langle p' | H_I^{(e,a)} | p \rangle &= \int \frac{dz}{2\pi\hbar} H_I^{(e,a)}(0) e^{i(p-p')z/\hbar} \\ &= \pm \frac{ieE_0 L_I p}{4\pi\gamma_0 m \hbar \omega} \text{sinc}\left(\frac{(p - p' \mp \hbar q_z) L_I}{2\hbar}\right) e^{i(p - p' \mp \hbar q_z)z/2\hbar} e^{\pm i\phi_0}, \end{aligned} \quad (18)$$

and then simplified to

$$\langle p' | H_I^{(e,a)} | p \mp p_{rec}^{(e,a)} \rangle = \pm \left(\frac{iv_0}{\pi}\right) \Upsilon \left(\frac{p \mp p_{rec}^{(e,a)}}{p_0}\right) \text{sinc}\left(\frac{\bar{\theta}_{e,a}}{2}\right) e^{i\frac{\bar{\theta}_{e,a}}{2} \mp i\phi_0}, \quad (19)$$

with

$$\Upsilon = \frac{eE_0 L_I}{4\hbar\omega}, \quad (20)$$

$$\bar{\theta}_{e,a} = \bar{\theta} \pm \frac{\varepsilon}{2}, \quad (21)$$

where  $\bar{\theta} = \left( \frac{\omega}{v_0} - q_z \right) L_I$  is the classical “interaction detuning parameter” and

$\varepsilon = \delta \left( \frac{\omega}{v_0} \right) L_I = 2\pi\delta L_I / \beta_0 \lambda$  is the interaction-length quantum recoil parameter.

We now can calculate the electron momentum density distribution after interaction:

$$\begin{aligned} \rho(p') &= \rho^{(0)}(p') + \rho^{(1)}(p') + \rho^{(2)}(p') \\ &= \frac{\left| c^{(0)}(p') \right|^2 + 2\text{Re}\{c^{(1)*}(p')c^{(0)}(p')\} + \left| c^{(1)}(p') \right|^2}{\int dp' \left( \left| c^{(0)}(p') \right|^2 + \left| c^{(1)}(p') \right|^2 \right)}, \end{aligned} \quad (22)$$

where

$$\rho^{(0)}(p') = \left| c^{(0)}(p') \right|^2 = \left( 2\pi\sigma_{p_0}^2 \right)^{-\frac{1}{2}} \exp \left( -\frac{(p-p_0)^2}{2\sigma_{p_0}^2} \right), \quad (23)$$

is the initial Gaussian momentum density distribution. The second and third terms are given by

$$\begin{aligned} \rho^{(1)}(p') &= \frac{2\text{Re}\{c_{p'}^{(1)(e)*}c_{p'}^{(0)} + c_{p'}^{(1)(a)*}c_{p'}^{(0)}\}}{\int dp' \left( \left| c^{(0)}(p') \right|^2 + \left| c^{(1)}(p') \right|^2 \right)} \\ &= \frac{2Y}{1+Y^2 \left( \text{sinc}\left(\frac{\bar{\theta}_e}{2}\right) + \text{sinc}\left(\frac{\bar{\theta}_a}{2}\right) \right)} \text{Re} \left\{ \left( \frac{p' - p_{rec}^e}{p_0} \right) \left( 2\pi\sigma_{p_0}^2 \right)^{-\frac{1}{2}} e^{\frac{(p'-p_0)^2}{4\bar{\sigma}_p^2(t_D)} - \frac{(p'-p_0-p_{rec}^e)^2}{4\bar{\sigma}_p^2(t_D)}} \times \right. \\ &\quad \left. \text{sinc}\left(\frac{\bar{\theta}_e}{2}\right) e^{i\left(\frac{\bar{\theta}_e}{2} + \phi_0\right)} - \left( \frac{p' + p_{rec}^a}{p_0} \right) \left( 2\pi\sigma_{p_0}^2 \right)^{-\frac{1}{2}} e^{\frac{(p'-p_0)^2}{4\bar{\sigma}_p^2(t_D)} - \frac{(p'-p_0+p_{rec}^a)^2}{4\bar{\sigma}_p^2(t_D)}} \text{sinc}\left(\frac{\bar{\theta}_a}{2}\right) e^{i\left(\frac{\bar{\theta}_a}{2} - \phi_0\right)} \right\}, \end{aligned} \quad (24)$$

and

$$\begin{aligned}\rho^{(2)}(p') = \Upsilon^2 & \left[ \left( \frac{p' + p_{rec}^e}{p_0} \right)^2 \rho^{(0)}(p' + p_{rec}^e) - \rho^{(0)}(p') \right] \text{sinc}^2 \left( \frac{\bar{\theta}_e}{2} \right) \\ & + \Upsilon^2 \left[ \left( \frac{p' - p_{rec}^a}{p_0} \right)^2 \rho^{(0)}(p' - p_{rec}^a) - \rho^{(0)}(p') \right] \text{sinc}^2 \left( \frac{\bar{\theta}_a}{2} \right).\end{aligned}\quad (25)$$

First we draw attention to the second order density distribution where the two terms in  $\rho^{(2)}$  display two side bands proportional to the initial density distribution  $\rho^{(0)}$  shifted centrally to  $p_0 \mp p_{rec}^{(e,a)}$  due to photon emission and absorption recoils (see Figure 2). Its first order moment results in the momentum acceleration/deceleration associated with stimulated radiative interaction:

$$\Delta p^{(2)} = \int \rho^{(2)}(p') p' dp' = \Upsilon^2 \left( \frac{\hbar \omega}{v_0} \right) \left[ \text{sinc}^2 \left( \frac{\bar{\theta}_e}{2} \right) - \text{sinc}^2 \left( \frac{\bar{\theta}_a}{2} \right) \right]. \quad (26)$$

Remarkably Equation (26) is independent of the wavepacket distribution  $\rho^{(0)}$ , and satisfactorily consistent with the stimulated emission/absorption terms in the quantum-electrodynamic radiative emission expression for a single plane-wave electron wavefunction in the limit  $\rho^{(0)}(p') = \delta(p - p')$  [11]:

$$\frac{dv_q}{dt} = \Gamma_{sp} \gamma_0 v_0 \left[ (v_q + 1) \frac{1}{\gamma_e v_e} \text{sinc}^2 \left( \frac{\bar{\theta}_e}{2} \right) - v_q \frac{1}{\gamma_e v_e} \text{sinc}^2 \left( \frac{\bar{\theta}_a}{2} \right) \right]. \quad (27)$$

Using Equation (26-27) in the conservation of energy and momentum relation,

$$\Delta p^{(2)} = - \frac{L_I}{v_0} \left( \frac{\hbar \omega}{v_0} \right) \left( \frac{dv_q}{dt} \right)_{st}, \quad (28)$$

We can relate the interaction parameter  $\Upsilon$  (Equation (20)) to the spontaneous radiation emission coefficient  $\Gamma_{sp}$

$$\Upsilon^2 = \frac{L_I}{v_0} \Gamma_{sp} v_q, \quad (29)$$



and derive an explicit expression for the spontaneous emission rate per mode  $\Gamma_{sp}$  from the relation between  $v_q$  and  $|E_0|^2$ .

It is also interesting to point out that in the limit of negligible recoil relative to the finite-length homogeneous line broadening limit [11]:

$$\varepsilon = \pi \frac{\hbar\omega}{m^* v_0^2} \frac{L_I}{\beta_0 \lambda} \ll 1, \quad (30)$$

$$\Delta p^{(2)} = \Upsilon^2 \frac{\hbar\omega}{v_0} \varepsilon \frac{d}{d\theta} \sin^2(\bar{\theta}/2), \quad (31)$$

consistently with the conventional classical gain expression of Smith-Purcell Cerenkov – FEL, as well as other FELs[9].

Note that according to Equation (26-28) there is no net second order acceleration (neither stimulated emission/absorption) at exact synchtonizm- $\bar{\theta} = 0$ . However, at the condition that the quantum recoil momentum  $p_{rec}^{(0)}$  is significant relative to the wavepacket momentum spread

$$p_{rec}^{(0)} = \frac{\hbar\omega}{v_0} \gg \sigma_{p0}, \quad (32)$$

the final momentum distribution in Equation (25) develops symetric sidebands, spaced  $\hbar\omega/v_0$  apart – see Figure 2. When higher order interaction results in multiphoton emission absorption – as in Feist *et al*'s experiment [21] multiple sidebands appear. In the classical limit of small recoil the multiple photon emission/absorption sidebands degenerate into a continuous broadening of the momentum probability distribution.

It is necessary to realize that the convential technology of electron energy spectroscopy necessitates averaged measurement of a multitude of electrons, in order to view the momentum distribution. If the electrons are emitted from a cathode unfiltered, then even if all emitted wavepacket are identical in their dimension, still the ensemble

average involves convolution with the initial (thermal) momentum distribution of single electron emission

$$\rho_{en} = \int \rho^{(0)}(p', p_0) f\left(\frac{p_0 - p_{0,en}}{\sigma_{p,th}}\right) dp_0, \quad (33)$$

(see Figure 2). This, necessarily, results in widening of the measurable standard deviation of the Gaussian distribution of the ensemble to  $\sigma_{p,en}$ :

$$\sigma_{p,en}^2 = \sigma_{p,th}^2 + \sigma_{p_0}^2. \quad (34)$$

Since the measurable distribution satisfies  $\sigma_{p,en} > \sigma_p$ , the wavepacket broadening cannot be distinguished from the thermal distribution that determines the so called “Coherence time” of electron microscopes  $t_{coh} = \hbar / 2\sigma_{E,en}$  (typically  $\sigma_{E,en} < 0.7 eV$ ). However, the quantum recoil effect on the momentum distribution of both emission and absorption (Equation (25)) is still observable if  $p_{rec}^{(0)} > \sigma_{p,en}$ . Figure 2 displays the measurable second order momentum density distribution (Equation (25)) for  $\theta_{0,en} = \left(\frac{\omega}{v_{0,en}} - q_z\right)L_I = 0$  and  $\varepsilon \ll 0$ . Sidebands are observable similarly to [21], but contrary to that experiment, in the framework of the first order perturbation theory, only two sidebands are observable corresponding to single photon emission/absorption. Note that the second order perturbation term lost the dependence on the phase  $\phi_0$  of the wavepacket center relative to the laser field, and therefore does not reveal any specific features of the single electron wavepacket.

We now draw attention to the first order density distribution (Equation (24)). This term has not been considered in previous analyses, but it is most interesting, because it retains the dependence on the phase  $\phi_0$ . In the limit of negligible recoil  $\varepsilon = 0$ , one obtains

$$\rho^{(1)}(p') = \frac{2\pi\Upsilon e^{-\Gamma^2/2} \text{sinc}\left(\frac{\bar{\theta}}{2}\right)}{1 + 2\Upsilon^2 \text{sinc}^2\left(\frac{\bar{\theta}}{2}\right)} \cos\left(\frac{\bar{\theta}}{2} - \phi_0 + \varphi\right) \left|C_{p'}^{(0)}\right|^2$$

$$\left( (p' - p_{rec}^e) e^{-\left(\frac{p' - p_0}{2\sigma_{p_0}^2}\right) p_{rec}^e + \delta\Gamma^2} - (p' + p_{rec}^a) e^{\left(\frac{p' - p_0}{2\sigma_{p_0}^2}\right) p_{rec}^a - \delta\Gamma^2} \right), \quad (35)$$

where

$$\varphi = \frac{2\omega t_D}{mv_0} (p' - p_0), \quad (36)$$

$$\Gamma = \frac{\omega}{v_0} \sigma_z(t_D) = \frac{2\pi\sigma_z(t_D)}{\beta\lambda}. \quad (37)$$

The decay coefficient  $e^{-\Gamma^2/2}$  assures that the first order term of the momentum distribution  $\rho^{(1)}$  is diminished when  $\Gamma \gg 1$ , namely when the wavepacket expands on its way from the source beyond the size of the interaction wavelength.

To first order in  $p_{rec}^{(0)}$ , we get

$$\rho^{(1)}(p') = \frac{4\left(\frac{\hbar\omega/v_0}{p_0}\right) \Upsilon \rho^{(0)}(p') \text{sinc}\left(\frac{\bar{\theta}}{2}\right) e^{-\Gamma^2/2}}{1 + 2\Upsilon^2 \text{sinc}^2\left(\frac{\bar{\theta}}{2}\right)} \cos\left(\frac{\bar{\theta}}{2} + \phi_0 + \varphi\right) \left[ 1 + \frac{\Gamma^2 p'}{2m^* v_0} - \frac{(p' - p_0) p'}{2\sigma_{p_0}^2} \right]. \quad (38)$$

Neglecting  $\varphi$ , the momentum transfer is:

$$\Delta p^{(1)} = \int \rho^{(1)}(p') p' dp' = \frac{\frac{2}{\gamma_0^2} \frac{\hbar\omega}{v_0} \Upsilon \text{sinc}\left(\frac{\bar{\theta}}{2}\right) \Gamma^2 e^{-\Gamma^2/2}}{\left(1 + 2\Upsilon^2 \text{sinc}^2\left(\frac{\bar{\theta}}{2}\right)\right)} \cos\left(\phi_0 + \frac{\bar{\theta}}{2}\right)$$

$$\simeq \frac{\Gamma^2 e^{-\Gamma^2/2}}{2\gamma_0^2} \frac{eE_0 L_I}{v_0} \text{sinc}\left(\frac{\bar{\theta}}{2}\right) \cos\left(\phi_0 + \frac{\bar{\theta}}{2}\right), \quad (39)$$

for  $\Upsilon \ll 1$ . This expression can be contrasted with the classical “point particle” momentum transfer equation

$$\Delta p_{point} = \frac{eE_0 L_I}{v_0} \text{sinc}\left(\frac{\bar{\theta}}{2}\right) \cos\left(\phi_0 + \frac{\bar{\theta}}{2}\right). \quad (40)$$

and the corresponding expression for stimulated superradiant emission  $W_q = v_0 \Delta p_{point}$  [22]. Except for the decay factor the acceleration/deceleration of the quantum wavepacket scales with  $\bar{\theta}$  and  $\phi_0$  similarly to the case of a point particle. Figures 3 and 4 display the momentum density distribution  $\rho^{(0)} + \rho^{(1)}$  for the case  $\bar{\theta} = 0$  and acceleration phase:  $\phi_0 = 0$ . The resultant post-interaction distribution gets lopsided towards positive momentum. The peak distribution is shifted about  $\Delta p^{(1)} = \frac{2}{\gamma_0^2} \frac{\hbar \omega}{v_0} \Upsilon$  for

$\Gamma = \sqrt{2}$ . Larger shift is not to be expected in our first order perturbation theory (classical acceleration/deceleration involves multiphoton exchange and requires complete high order perturbation analysis of Equation (1) or numerical computation [23]). A left shifted momentum distribution would appear in the case of deceleration for phase  $\phi_0 = \pi$ .

Of great curiosity is the effect of the wavepacket expansion factor  $\Gamma$  in Equation (38-39). Evidently the “point particle” limit (40) does not evolve from Equation (39) in the limit  $\Gamma \ll 1$  ( $\sigma_z(t_D) \ll \lambda \beta_0$ ) as might be expected. Figure 5 shows that the decay factor  $\Gamma^2 e^{-\Gamma^2/2}$  diminishes in the limits  $\Gamma \rightarrow 0$ ,  $\Gamma \rightarrow \infty$ , it reaches a maximum value  $2/e$  when  $\Gamma = \sqrt{2}$ . Substitution of Equation (9) in Equation (13) results in the relation

$$\sigma_z(t_D) = \sqrt{\sigma_{z0}^2 + \left(\frac{\lambda_c^*}{4\pi} \frac{ct_D}{\sigma_{z0}}\right)^2}, \quad (41)$$

It is obvious that  $\sigma_{z_0} \rightarrow 0$  is not the point particle limit, since then the wavepacket size explodes. Moreover,  $\sigma_z(t_D)$  cannot be arbitrarily small, it has an absolute minimum for any given  $t_D$ , independently of  $\sigma_{z_0}$

$$\sigma_z(t_D)|_{\min} = \sqrt{\frac{\lambda_c^*}{2\pi} c t_D}, \quad (42)$$

This corresponds to a minimum value of  $\Gamma$  for fixed frequency  $\omega$

$$\Gamma_{\min} = \frac{\omega}{v_0} \sqrt{\frac{\lambda_c^*}{2\pi} c t_D}, \quad (43)$$

We define a critical drift length  $z_G = v_0 t_{DG}$  as the distance for which  $\Gamma_{\min} = \sqrt{2}$

$$z_G = \frac{\beta_0^3 \gamma_0^3}{\pi} \frac{\lambda^2}{\lambda_c}, \quad (44)$$

We come to the significant observation that for drift distances away from the source  $L_D \gg z_G$ , phase-dependent linear (in the field) acceleration/deceleration of a single electron is diminished, because the wavepacket inevitably spreads wider than the interacting wavelength, and its phase is undefined even if one can determine accurately the wavepacket emission time relative to the wave phase  $\phi_0$  at the interaction region. This observation is also consistent with an earlier suggestion that the quantum wavepacket spread poses a fundamental physical high frequency limit or short wavelength limit  $\lambda_{\text{cutoff}} = (\pi \lambda_c / \beta^3 \gamma^3)^{1/2}$  on measurement of particle beam shot-noise, challenging the conventional mathematical “point-particle” model presentation of shot-noise as an unbound “white noise” [24].

The diminishing of the linear field acceleration due to the  $\Gamma^2 e^{-\Gamma^2/2}$  factor is quite understandable in the limit  $\Gamma \gg \sqrt{2}$  that corresponds to wavepacket spread beyond the accelerating field wavelength  $\sigma_z(t_D) \gg \beta_0 \lambda$ . On the other hand, the diminishing

acceleration effect in the limit  $\Gamma(t_D) \ll 1$  due to the factor  $\Gamma^2 e^{-\Gamma^2/2}$  (that is not forbidden in the range  $L_D < z_G$ ) is in contradiction to the intuitive expectation that in this limit,  $\sigma_z(t_D) \ll \beta_0 \lambda$ , the wavepacket would accelerate as a point particle. However we must point out that this result was derived within the framework of first order perturbation theory, where only single photon recoil is involved in the radiative interaction.

The phase-dependent linear field acceleration regime  $\Delta p^{(1)}$  is of fundamental interest, because contrary to the second order acceleration  $(\rho^{(2)}, \Delta p^{(2)})$ , its characteristics depend on the wavepacket dimensions. So far, previous laser acceleration experiments of single electrons [10,21] were carried out only in the second order acceleration regime, where only broadening of the momentum spectrum is possible without net acceleration.

Inspection of Equation (39) indicates that maximum acceleration (or deceleration) would take place for  $\bar{\theta} = 0, \phi_0 = 0(\text{or } \pi), \Gamma(t_D) = \sqrt{2}$  :

$$\Delta p_{\max}^{(1)} = \frac{4}{e\gamma_0^2} \Upsilon p_{\text{rec}}^{(0)}, \quad (44)$$

where  $\Upsilon$  - the number of exchanged photons (Equation (20)) must satisfy  $\Upsilon < 1$  in the first order approximation, and  $p_{\text{rec}}^{(0)} = \hbar\omega/v_0$ . Therefore, net acceleration is achievable, but because

$$\Gamma(t_D) > \Gamma(t_D = 0) = \Gamma_0 = \frac{\omega}{v_0} \sigma_{z_0} = \frac{p_{\text{rec}}^{(0)}}{\sigma_{p_0}}, \quad (45)$$

therefore the acceleration  $\Delta p_{\max}^{(1)}$  is smaller than the wavepacket momentum spread  $\sigma_{p_0}$  and the relative shift of the momentum distribution is marginally observable (as displayed in Figure 3). The relative shift may however be larger than 1 in the multiphoton exchange regime where  $\Upsilon \gg 1$ .

We consider briefly the feasibility of a phase-dependent laser acceleration experiment. Assume electrons are photo-emitted from a tip, accelerated to 120MeV ( $\beta_0 = 0.7, \gamma_0 = 1.4$ ), and energy filtered to  $\sigma_E = 0.1\text{eV}$  [25] (corresponding to  $\sigma_z > \sigma_{z0} > 0.5\mu\text{m}$ ). Sub 500 attoSecond single electron wavepacket emission has already been demonstrated by Kruger *et al* [26], so that phase synchronization with an acceleration IR laser beam (sub-harmonic of the photo-emission laser, an OPO or a THz beam [27]) is feasible. If we consider an example of  $\lambda = 6\mu\text{m}$  ( $\lambda\beta_0 = 4.2\mu\text{m}$ ), then  $z_G = 48\text{cm}$ . Performing the laser interaction within  $L_D < z_G$ , then net acceleration dependent on  $\sigma_{z0}$  may be detectable for the above parameters ( $\sigma_z > \sigma_{z0} > 0.5\mu\text{m}$ ), so that  $0.75 < \Gamma(t_D, \sigma_{z0}) < \sqrt{2}$  and the attenuation range (for single photon exchange) is  $0.42 < \Gamma^2 e^{-\Gamma^2/2} < 2/e$ .

Here we raise the question if a phase-dependent acceleration experiment can be used to characterize the wavepacket size of electrons, photo-emitted from a single electron emission source like a tip [26] or an ion cold-trap [28]. We believe that the wavepacket size is a real physical parameter that is determined by the material or atom structure and temperature, and by the emission process (tunneling, photoemission). Unfortunately, the measurement of acceleration and momentum distribution requires repeated measurement of a multitude of particles (we note that according to [29] this is a technological limitation and may possibly avoided by weak measurements[30]). In this case, in measurement of an ensemble of electrons, the acceleration effect may be masked by the thermal distribution of the single particle center momentum (see Equation (34)).

In conclusion, the analysis presented here shows that stimulated interaction of a wavepacket with radiation (contrary to spontaneous emission) can be dependent on the features of the wavepacket in a certain range. Our semiclassical analysis describes the stimulated radiative interaction of a single electron wavepacket in the ranges of transition between the quantum to classical limits and independently between the finite-size wavepacket to point-particle limit. We identified conditions for realizing linear field

acceleration/deceleration of a wavepacket that is dependent on the wavepacket envelope size and phase. In this range of operation, net acceleration of a single electron wavepacket is possible. So far laser acceleration and PINEM experiments have not been carried out in this regime and therefore such net acceleration has not been observed. In the first order perturbation theory the acceleration is small relative to the wavepacket momentum spread. It can be large in the multiphoton exchange limit as in point particle acceleration. We discussed the limitation of using the wavepacket-dependent acceleration scheme for measuring the characteristic wavepacket size of electrons, emitted from a specific electron source. If the measurement requires averaging over multiple electrons the measurement may be limited by the classical thermal velocity spread of the particles ensemble.



**Acknowledgements** We acknowledge Yakir Aharonov, A. Friedman, S. Rushin and Amnon Yariv for useful discussions and comments. The work was supported in parts by DIP (German-Israeli Project Cooperation) and US-Israel Binational Science Foundation, and by the PBC program of the Israel council of higher education.

**Author Contributions** A.G. conceived and supervised the project. Y.P. performed modeling and numerical calculation of the electron wavepacket with the near-field interaction. A.G. and Y.P. co-wrote the paper with all authors contributing to discussion and preparation of the manuscript. Correspondance and requests for materials should be addressed to A. G. ([gover@eng.tau.ac.il](mailto:gover@eng.tau.ac.il)) or Y.P. ([yimingpan@smail.nju.edu.cn](mailto:yimingpan@smail.nju.edu.cn)).

**Competing interests statement** The authors declare no competing financial interest.

## References

1. Brau, Charles A. Modern Problems in Classical Electrodynamics. *Oxford University Press*, ISBN 0-19-514665-4 (2004).
2. H. Motz, "Applications of the radiation from fast electron beams", *J. Appl. Phys.* **22**, 527-535 (1951).
3. V. P. Sukhattmee, P. W. Wolff, "Stimulated Compton scattering as a radiation source-Theoretical limitations", *J. Appl. Phys.* **44**, 2331-2334 (1973).
4. Cherenkov, P. A., "Visible emission of clean liquids by action of  $\gamma$  radiation". *Doklady Akademii Nauk SSSR*. **2**, 451(1934).
5. V. L. Ginzburg and I. M. Frank, "Transition radiation," *Zh. Eksp. Teor. Fiz.* **16**, 15–22 (1946).
6. S. J. Smith and E. M. Purcell, "Visible light from localized surface charges moving across a grating," *Phys. Rev.* **92**, 1069 (1953).
7. J. M. Madey, "Stimulated emission of bremsstrahlung in a periodic magnetic field," *Appl. Phys.* **42**, 1906-1913 (1971).
8. Pellegrini, C., A. Marinelli, and S. Reiche. "The physics of x-ray free-electron lasers." *Reviews of Modern Physics* **88(1)**, 015006 (2016).
9. Gover, A., and P. Sprangle. "A unified theory of magnetic bremsstrahlung, electrostatic bremsstrahlung, Compton-Raman scattering, and Cerenkov-Smith-Purcell free-electron lasers." *IEEE Journal of Quantum Electronics* **17(7)**, 1196-1215 (1981).
10. Peralta, et al., Demonstration of electron acceleration in a laser-driven dielectric microstructure. *Nature* **503(7474)**, 91-94 (2013).
11. Friedman, A., Gover, A., Kurizki, G., Ruschin, S., & Yariv, A., Spontaneous and stimulated emission from quasifree electrons. *Reviews of Modern Physics* **60(2)**, 471 (1988).
12. Peter Kling et al., "What defines the quantum regime of the free-electron laser?" *New J. Phys.* **17**, 123019 (2015).

13. I. Kaminer, *et al.*, "Quantum Čerenkov radiation: spectral cutoffs and the role of spin and orbital angular momentum." *Phys. Rev. X* **6**, 011006 (2016).
14. I. P. Ivanov, "Quantum calculation of the Vavilov-Cherenkov radiation by twisted electrons" *Phys. Rev. A* **93**, 053825 (2016).
15. P. Krekora, R. E. Wagner, Q. Su, and R. Grobe, *Laser Phys.* **12**, 455 (2002).
16. E. A. Chowdhury, I. Ghebregziabihier, and B. C. Walker, *J. Phys. B* **38**, 517 (2005).
17. J. Peatross, J. P. Corson, and G. Tarbox, *Am. J. Phys.* **81**, 351 (2013).
18. A. Barut, *Found. Phys. Lett.* **1**, 47 (1988).
19. Ware, Michael, et al. "Measured photoemission from electron wave packets in a strong laser field." *Optics letters* **41(4)**, 689-692 (2016).
20. Peatross, Justin, et al. "Photoemission of a single-electron wave packet in a strong laser field." *Phys. Rev. Lett.* **100(15)**, 153601 (2008).
21. Feist, A. et al. Quantum coherent optical phase modulation in an ultrafast transmission electron microscope. *Nature* **521**, 200-203 (2015).
22. Gover, A., Superradiant and stimulated-superradiant emission in prebunched electron-beam radiators. I. Formulation. *Physical Review Special Topics-Accelerators and Beams*, **8(3)**, 030701(2005).
23. Talebi, Nahid. "Schrödinger electrons interacting with optical gratings: quantum mechanical study of the inverse Smith–Purcell effect." *New Journal of Physics* **18(12)**, 123006 (2016).
24. R. Iancu, A. Gover, A. Nause, "spectral limits and frequency sum-rule of current and radiation noise measurement" *TUP007 Proceedings of FEL*, Basel, Switzerland (2014).
25. Krivanek, Ondrej L., Tracy C. Lovejoy, Niklas Dellby, and R. W. Carpenter. "Monochromated STEM with a 30 meV-wide, atom-sized electron probe." *Microscopy* **2013**, 089 (2013).
26. Michael Kruger, Markus Schenk, Peter Hommelhoff, "Attosecond control of electrons emitted from a nanoscale metal tip", *Nature* **475**: 78 -81 (2011).

27. E Curry, S Fabbri, P Musumeci and A Gover, "THz-driven zero-slippage IFEL scheme for phase space manipulation" *New J. Phys.* **18**, 113045 (2016).
28. W.J. Engelen, E.J.D. Vredenburg, O.J. Luiten, "Analytical model of an isolated single-atom electron source" *Ultramicroscopy* **147**, 61–69 (2014).
29. Nicklaus, Marc, and Franz Hasselbach. "Wien filter: A wave-packet-shifting device for restoring longitudinal coherence in charged-matter-wave interferometers." *Phys. Rev. A* **48(1)**, 152(1993).
30. Aharonov, Yakir, and Lev Vaidman. "The two-state vector formalism: an updated review." In *Time in quantum mechanics*, 399-447. Springer Berlin Heidelberg (2008).

## Figures

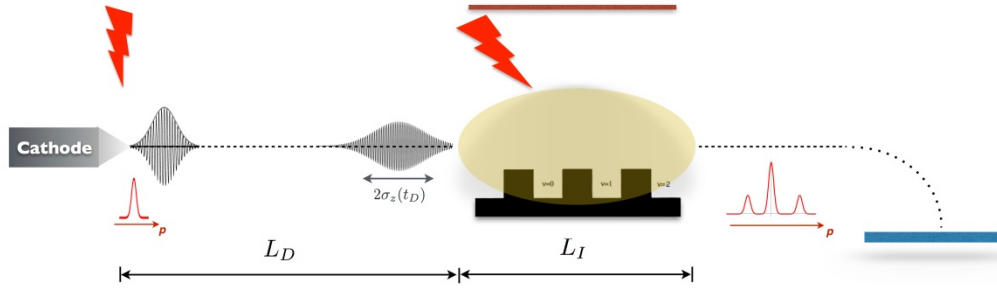


**Figure 1| The experiment setup.** Single electron wavepackets are photo-emitted from a cathode driven by an ultra-short pulse fSec laser. After a free propagation length  $L_D$ , the expanded wavepacket passes next to the surface of a grating of length  $L_I$ , and interacts with the near-field radiation, that is excited by an IR wavelength laser, phase locked to the photo-emitting laser. The accelerated/decelerated momentum distribution of the modulated wavepacket is measured with an electron energy spectrometer.

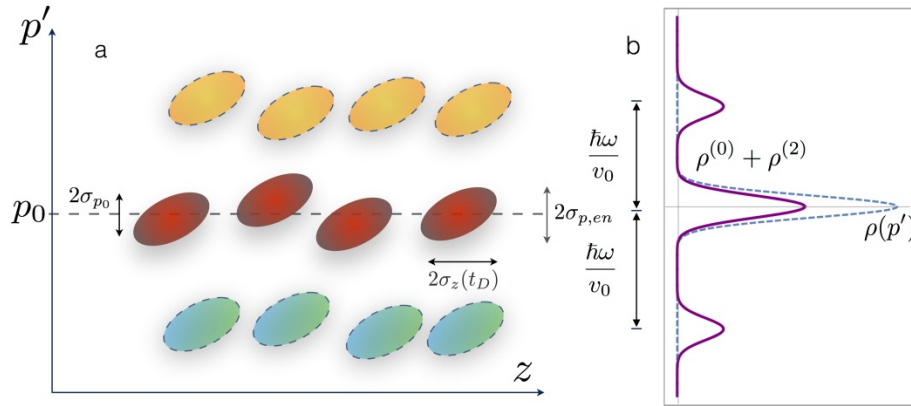


**Figure 2| The quantum recoil limit of electron-laser interaction.** The phase-space distribution of an ensemble of quantum wavepackets after interaction with the near-field is shown in (a), and its final momentum distribution is shown in (b). In this limit the

condition  $p_{rec} = \frac{\hbar\omega}{v_0} \gg \sigma_{en} > \sigma_{p0}$  is satisfied, where  $\sigma_{en}$  is the ensemble momentum spread.

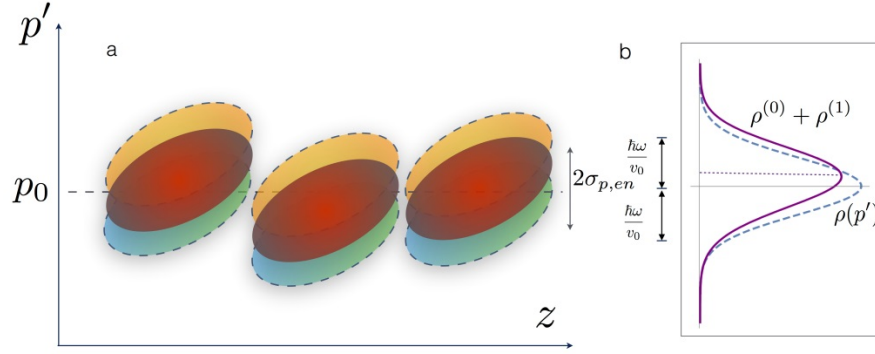


**Figure 3| Linear field acceleration of a phase-defined wavepacket.** The phase space distribution of electron quantum wavepackets interacting weakly with the near-field wave is shown in (a), and its final momentum distribution in (b). In this limit

$$\Gamma = \frac{2\pi\sigma_z(t_D)}{\beta\lambda} \approx 1 \text{ and } p_{rec} = \frac{\hbar\omega}{v_0} \ll \sigma_{p0}.$$

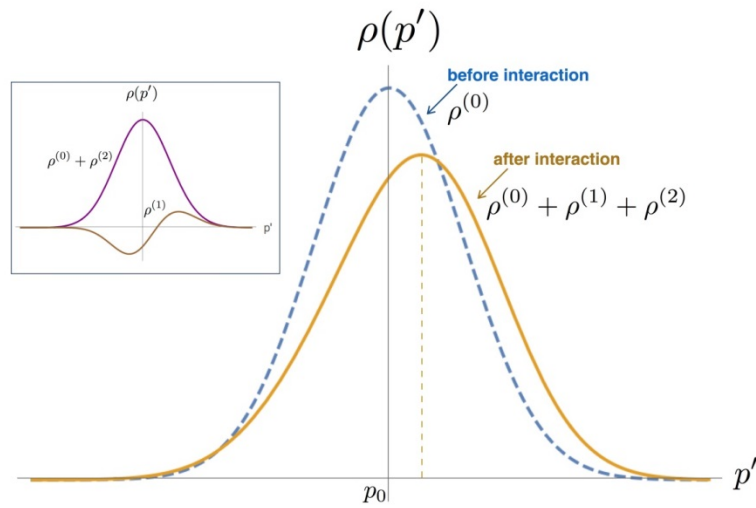


**Figure 4| Total final momentum distribution of a Linear field accelerated phase-defined wavepacket.** The parameters are for maximal momentum gain:  $\bar{\theta} = 0$  (velocity synchronizm),  $\phi_0 = 0$  (accelerating phase),  $\Gamma = \sqrt{2}$ . The inset shows the incremental distributions  $\rho^{(1)}$  and  $\rho^{(2)}$  seperately.

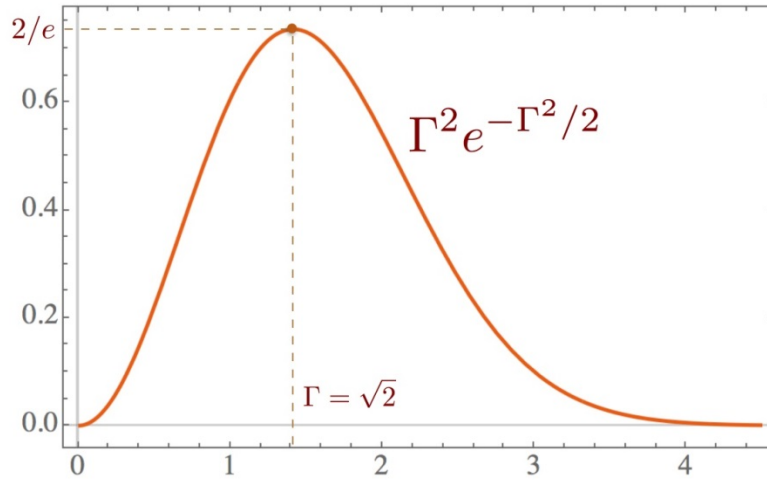


**Figure 5| The decay factor of wavepacket acceleration/deceleration relative to the “point-particle” classical case.** In both limits of short wavepacket ( $\Gamma \rightarrow 0$ ) and long wavepacket ( $\Gamma \rightarrow \infty$ ), the decay factor diminishes the acceleration/deceleration.

**Video-1:** Wavepacket evolution for the case  $\bar{\theta} = 0$  weak field

$\Upsilon \ll 1, \sigma_{p0} < \hbar\omega/v_0, \sigma_z(t_D) > \lambda\beta_0$  with sidebands formation and no net acceleration:

a) Evolution in space - z (pink -  $\text{Im } \Psi(z)$  , blue-  $\text{Re } \Psi(z)$  , purple -  $|\Psi(z)|$ ).

b) Evolution in momentum  $\rho(p) = |c(p)|^2$  .

**Video-2:** Wavepacket evolution for the case  $\bar{\theta} = 0, \phi_0 = 0/\pi$  , and strong field

$\Upsilon \gg 1, \sigma_z(t_D) < \lambda\beta_0$  with net acceleration/deceleration:

a) Evolution in space- z.

b) Evolution in momentum  $\rho(p) = |c(p)|^2$  .